GEOLOGY | THE GEOLOGICAL SOCIETY OF AMERICA®

https://doi.org/10.1130/G51211.1

Manuscript received 28 November 2022
Revised manuscript received 1 March 2023
Manuscript accepted 3 May 2023

Published online 16 May 2023

Breaking plates: Creation of the East Anatolian fault, the Anatolian plate, and a tectonic escape system

Donna L. Whitney[1,*], Jonathan R. Delph[2], Stuart N. Thomson[3], Susan L. Beck[3], Gilles Y. Brocard[4], Michael A. Cosca[5], Michael H. Darin[6,7], Nuretdin Kaymakcı[8], Maud J.M. Meijers[9], Aral I. Okay[10], Bora Rojay[8], Christian Teyssier[1], and Paul J. Umhoefer[7,†]

[1]Department of Earth & Environmental Sciences, University of Minnesota, Minneapolis, Minnesota 55455, USA
[2]Department of Earth, Atmospheric & Planetary Science, Purdue University, West Lafayette, Indiana 47907, USA
[3]Department of Geosciences, University of Arizona, Tucson, Arizona 85721, USA
[4]Maison de l'Orient et de la Méditerranée, University of Lyon 2, 69007 Lyon, France
[5]Denver Federal Center, U.S. Geological Survey, Denver, Colorado 80225, USA
[6]Oregon Department of Geology & Mineral Industries, Portland, Oregon 97232, USA
[7]Northern Arizona University, School of Earth & Sustainability, Flagstaff, Arizona 86011, USA
[8]Department of Geological Engineering, Middle East Technical University, 06800 Cankaya, Ankara, Turkey
[9]Institute of Earth Sciences, Karl-Franzens Universität, 8010 Graz, Austria
[10]Eurasia Institute of Earth Sciences, Istanbul Technical University, Maslak 34469, Istanbul, Turkey

ABSTRACT

Lateral movement of lithospheric fragments along strike-slip faults in response to collision (escape tectonics) has characterized convergent settings since the onset of plate tectonics and is a mechanism for the formation of new plates. The Anatolian plate was created by the sequential connection of strike-slip faults following ≥10 m.y. of distributed deformation that ultimately localized into plate-bounding faults. Thermochronology data and seismic images of lithosphere structure near the East Anatolian fault zone (EAFZ) provide insights into the development of the new plate and escape system. Low-temperature thermochronology ages of rocks in and near the EAFZ are significantly younger than in other fault zones in the region, e.g., apatite (U-Th)/He: 11–1 Ma versus 27–13 Ma. Young apatite (U-Th)/He ages and thermal history modeling record thermal resetting along the EAFZ over the past ~5 m.y. and are interpreted to indicate thermal activity triggered by strike-slip faulting in the EAFZ as it formed as a through-going, lithosphere-scale structure. The mechanism for EAFZ formation may be discerned from S-wave velocity images from the Continental Dynamics–Central Anatolian Tectonics (CD-CAT) seismic experiment. These images indicate that thin but strong Arabian lithospheric mantle extends ~50–150 km north beneath Anatolian crust and would have been located near the present surficial location of the Bitlis-Zagros suture zone (co-located with the EAFZ in our study area) at ca. 5 Ma. Underthrusting of strong Arabian lithosphere facilitated localization of the EAFZ and thus was a fundamental control on the formation of the Anatolian plate and escape system.

INTRODUCTION

The formation of a new tectonic plate occurs when lithospheric weak zones localize deformation (Tackley, 2000) and connect to create a block of fault-bounded lithosphere that moves in a direction distinct from that of the ancestral plate. Plate formation by this mechanism has likely occurred since the inception of plate tectonics, although this process can be documented only in opportune cases, such as the Anatolian plate. In this study, we show how and when the Anatolian plate was created from the Eurasian plate.

One mode of plate formation is associated with escape tectonics, a strike-slip–dominated regime of large-scale transport of lithosphere obliquely away from a convergent zone, as is occurring today in Anatolia, SE Asia and other regions related to India-Asia collision, the western Pacific, and the Caribbean (Burke and Şengör, 1986). The relative importance of push (collision) and pull (retreating subduction) in driving escape has long been debated (Tapponnier et al., 1982; Faccenna et al., 2013).

The Anatolian plate developed under near-ideal conditions for escape owing to components of push (Arabia-Eurasia collision) and pull (Aegean slab pull), assisted by favorably oriented lithospheric weak zones and rheological boundaries (Black Sea region lithosphere; Molnar and Dayem, 2010). Nevertheless, the development of the escape system was protracted: It took ≥10 m.y. after early to mid-Miocene Arabia-Anatolia collision (i.e., so-called "hard collision") for the East Anatolian fault zone (EAFZ) to form as a through-going fault. We evaluate the timing and contributing factors in the development of escape tectonics, with a focus on the EAFZ because its formation completed the escape system and created the Anatolian plate.

OVERVIEW OF ANATOLIAN TECTONICS

Anatolia was assembled by numerous subduction and collision events. Late Mesozoic–early Paleogene metamorphism, magmatism, and deformation were followed by extension in the west, collision in the east, slab tearing/break-off below central and eastern Anatolia, extension-driven exhumation of midcrustal rocks, episodic and voluminous volcanism, and

Donna L. Whitney https://orcid.org/0000-0002-8296-4692
*dwhitney@umn.edu
†Deceased

CITATION: Whitney, D.L., et al., 2023, Breaking plates: Creation of the East Anatolian fault, the Anatolian plate, and a tectonic escape system: Geology, v. 51, p. 673–677, https://doi.org/10.1130/G51211.1

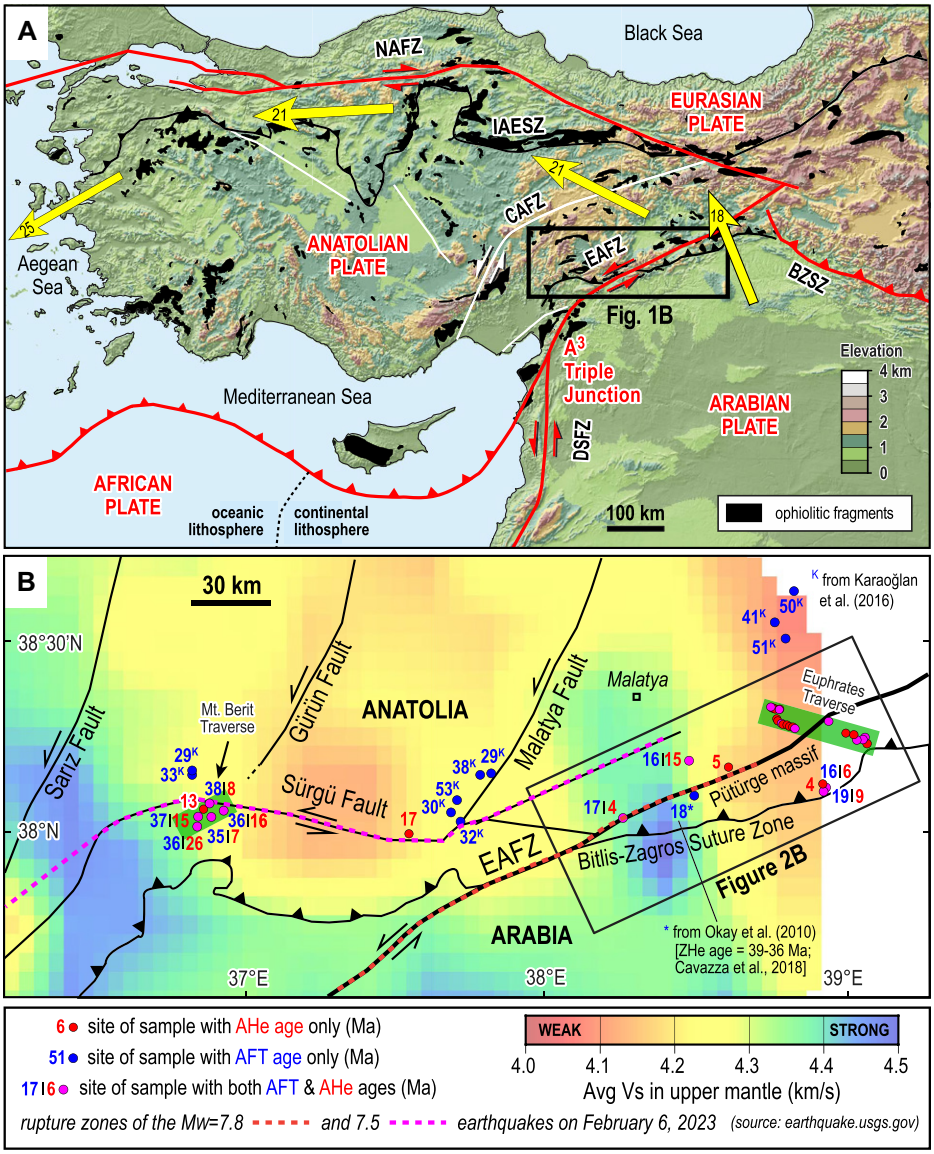

Figure 1. (A) Topographic map of Anatolian region showing major structures: A³—Anatolia-Arabia-Africa triple junction; BZSZ—Bitlis-Zagros suture zone; CAFZ—Central Anatolian fault zone; DSFZ—Dead Sea fault zone; EAFZ—East Anatolian fault zone; IAESZ—İzmir-Ankara-Erzincan suture zone; NAFZ—North Anatolian fault zone. Yellow arrows—representative global positioning system velocities relative to Eurasia (in mm/yr; Reilinger et al., 2006). (B) Map of field area with major structures and apatite fission-track (AFT) and apatite (U-Th)/He (AHe) ages (in Ma); ZHe ages are not shown (see Fig. 2). Green rectangles show two traverses: East Anatolian fault zone and Mount Berit. Background shows average S-wave velocity for upper 30 km of mantle (Delph et al., 2017).

uplift of a plateau and mountain ranges (Schildgen et al., 2014; Okay et al., 2020).

Arabia-Eurasia convergence was a driver of the escape system. Collision resulted in widespread deformation, with effects as far west as the Central Anatolian fault zone (Fig. 1A; Umhoefer et al., 2020). Low-temperature thermochronology from the Bitlis-Zagros suture zone (BZSZ) and the timing of Miocene marine carbonate sedimentation indicate complete closure of a marine basin by ca. 20 Ma (Okay et al., 2010; Cavazza et al., 2018).

Evidence from faults and other deformation features across central/eastern Anatolia indicates a transition from approximately N-S regional transpression to N-S compression accommodated by approximately E-W extension from ca. 25 to 5 Ma (Kaymakçı et al., 2010; Umhoefer et al., 2020). A subducted slab below Anatolia experienced tearing and break-off at ca. 13–11 Ma, corresponding to volcanism in central and eastern Anatolia and uplift of the Tauride Mountains (e.g., Meijers et al., 2018).

The boundaries of the Anatolian plate are the conjugate North and East Anatolian fault zones and a megathrust accommodating subduction of African lithosphere in the west and south (Fig. 1A). The timing of faulting has been determined by a variety of methods, including dating volcanic rocks in fault zones. The >1200-km-long dextral North Anatolian fault zone (NAFZ) formed by ca. 15–11 Ma in the east and propagated to the west (Şengör et al., 2005). There have been fewer studies of the ~700-km-long EAFZ. A wide range of ages has been proposed, but most estimates are Pliocene (McKenzie, 1976; Muehlberger and Gordon, 1987; Rojay et al., 2001; Cosca et al., 2021). The EAFZ exhibits transpression and transtension segments in a dominantly sinistral strike-slip system (Duman and Emre, 2013).

To evaluate the age of the EAFZ, formation of the Anatolian plate, and inception of escape tectonics, we obtained low-temperature thermochronology data from metamorphic and intrusive rocks in and near the EAFZ and other major faults, and we evaluated these data in the context of seismic images that illuminate lithosphere structure.

LOW-TEMPERATURE THERMOCHRONOLOGY RESULTS AND MODELING

Results

We present apatite fission-track (AFT) ages from 14 samples and 109 apatite and 12 zircon single-grain (U-Th)/He (AHe and ZHe) ages from 23 and 4 samples, respectively, including 21 samples from a NW-SE traverse of Late Cretaceous metamorphic rocks of the Pütürge massif across the EAFZ near where the Euphrates River is displaced by the fault (Figs. 1B and 2; for methods and full data set, see Supplemental Material[1] and Tables S2–S5). These thermochronometers record cooling <~200–160 °C (ZHe), ~120–100 °C (AFT), and ~70–50 °C (AHe) for cooling rates of 1–10 °C/m.y.

AFT ages near the EAFZ are between 22 and 11 Ma (Figs. 1B and 2; Tables S2–S3). In the near-Euphrates traverse, AFT ages (ca. 16–10 Ma) are similar over ~1400 m in elevation change, consistent with rapid mid-Miocene cooling. This matches the time of rapid cooling reported in thermochronologic studies along the BZSZ to the east (Okay et al., 2010; Cavazza et al., 2018), interpreted as recording increased exhumation rates related to mid-Miocene hard collision.

AHe data show significant intrasample age dispersion with no correlation of age versus U and Th concentration and/or grain size. In the absence of such correlations, age dispersion in rapidly cooled samples is most likely caused

[1]Supplemental Material. S1: Description of thermochronology methods and associated references. Tables S2–S5. S6-8: Maximum Mode thermal history. S6-9: Summary of graphical QTQt inverse thermal modeling plots. Figures S6–S10. Please visit https://doi.org/10.1130/GEOL.S.22756583 to access the supplemental material, and contact editing@geosociety.org with any questions.

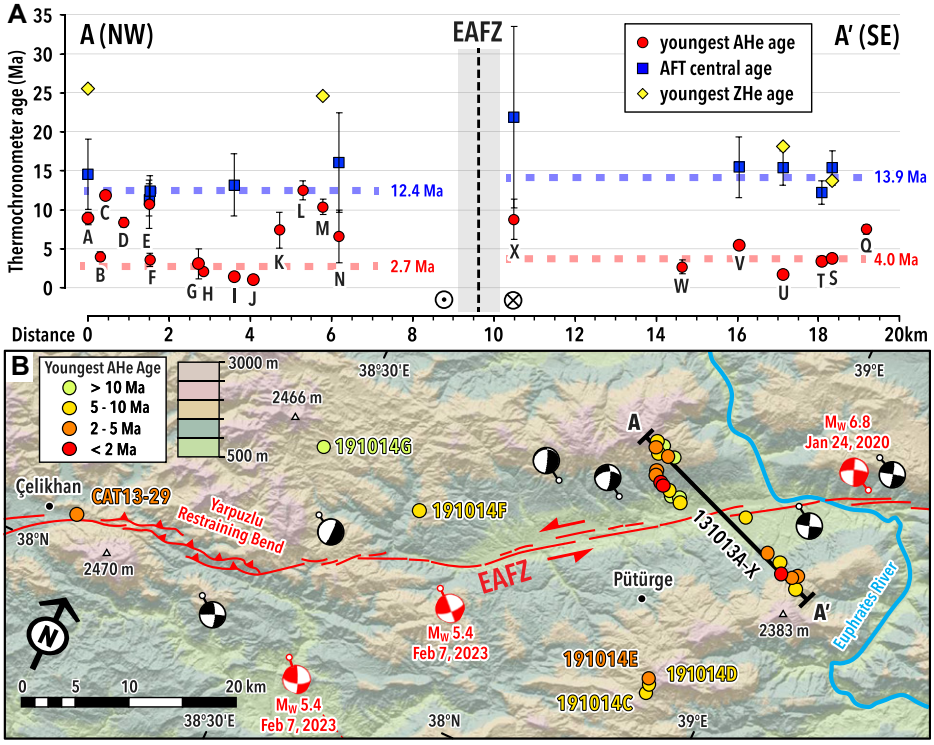

Figure 2. (A) Age-distance plot for thermochronology data from East Anatolian fault zone (EAFZ) traverse near Euphrates River. Letters are part of sample numbers with prefix 131013. Dashed lines indicate weighted means: blue—apatite fission-track (AFT) mean age; red—apatite (U-Th)/He (AHe) mean age. ZHe—zircon (U-Th)/He age. (B) Relief map near East Anatolian fault zone with sample locations color-coded by youngest AHe ages. Earthquake focal mechanisms are from Bulut et al. (2012) (black), with recent data for some M > 5 events (source: https://www.emsc-csem.org/).

by excess He such that the AHe grain age of the youngest sample represents the time of fast cooling (He et al., 2021; Tables S2 and S4). In our study, the youngest AHe grain ages mostly range from 15 to 5 Ma, with very young ages (<3 Ma) only in the EAFZ.

Single-grain ZHe ages from the near-Euphrates traverse are between 35 and 14 Ma (Fig. 2; Tables S2 and S5). ZHe ages SE of the EAFZ are younger (26–14 Ma) than those on the NW side (35–25 Ma), with the latter being slightly younger than ca. 39–36 Ma ZHe ages reported by Cavazza et al. (2018) ~10 km SW of the traverse (Fig. 1B).

Thermal History Modeling

We conducted inverse thermal history modeling (QTQt) on samples with age data from multiple thermochronometers, including multisample modeling from three traverses over a range of elevations (Figs. 3A–3C; Supplemental Material S1 and Figs. S6–S9). Nearly all modeling results support rapid cooling through the AFT partial annealing zone ca. 18–12 Ma, as previously reported along the BZSZ to the east (Okay et al., 2010; Cavazza et al., 2018). To predict the very young AHe ages from the EAFZ traverse, the modeling results favor a period of short-lived reheating followed by rapid cooling to surface temperatures over the past ~5–4 m.y. confined to the EAFZ. Modeling results from other parts of the Pütürge massif and Mount Berit to the west of the EAFZ (Figs. 3B–3C) show only steady Pliocene to Pleistocene cooling.

SEISMIC IMAGING: LITHOSPHERIC STRUCTURE OF THE EAST ANATOLIAN FAULT ZONE

The crust and upper-mantle structure in and near the EAFZ is revealed by S-wave velocities derived from joint inversion of P-wave receiver functions and Rayleigh wave dispersion data (Abgarmi et al., 2017; Delph et al., 2017). Results show that the western half of the EAFZ cuts through a region underlain by fast S-wave velocities (~4.4–4.6 km/s; Figs. 1B and 4). These velocities are more consistent with Arabian plate lithospheric mantle (~4.5 km/s) than velocities of Anatolian lithospheric mantle (~4.2 km/s), despite lying ~50–150 km N of the surface expression of the BZSZ (Figs. 1B and 4;

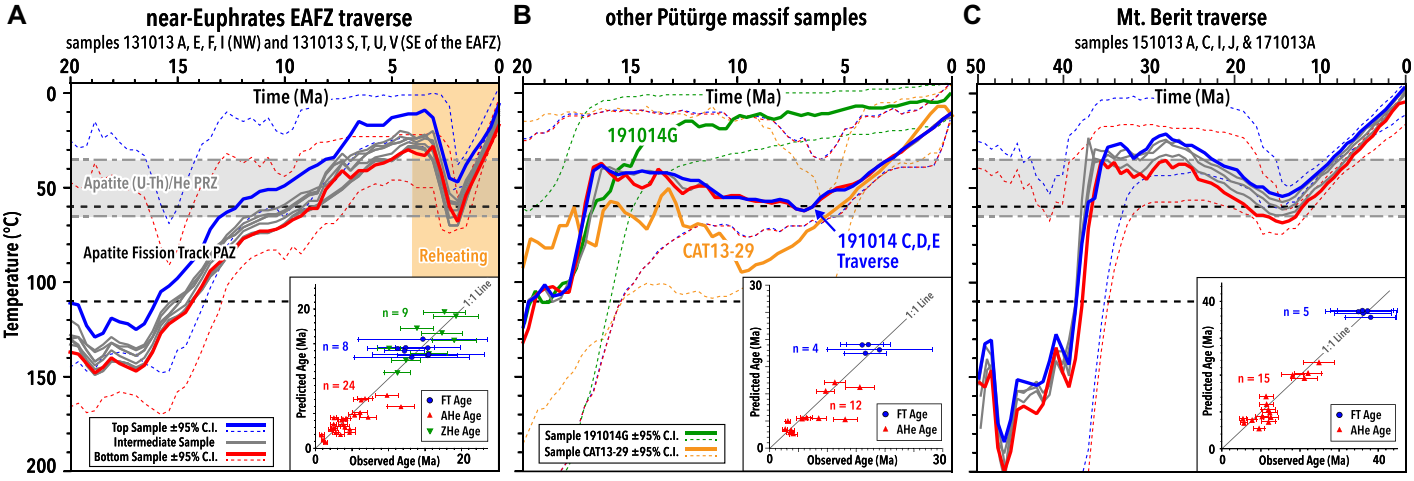

Figure 3. (A–C) Temperature-time plots (all at same scale) showing inverse thermal history models for (A) East Anatolian fault zone traverse (EAFZ; data from eight samples: four on each side of EAFZ, all with both apatite fission-track [FT] and [U-Th]/He [AHe] data; three also have zircon [U-Th]/He [ZHe] data); (B) other samples in region; and (C) samples from Mount Berit traverse (Fig. 1B). Thick lines show expected (weighted mean) thermal history with 95% credible intervals (C.I.; dashed lines). PRZ—partial resetting zone; PAZ—partial annealing zone.

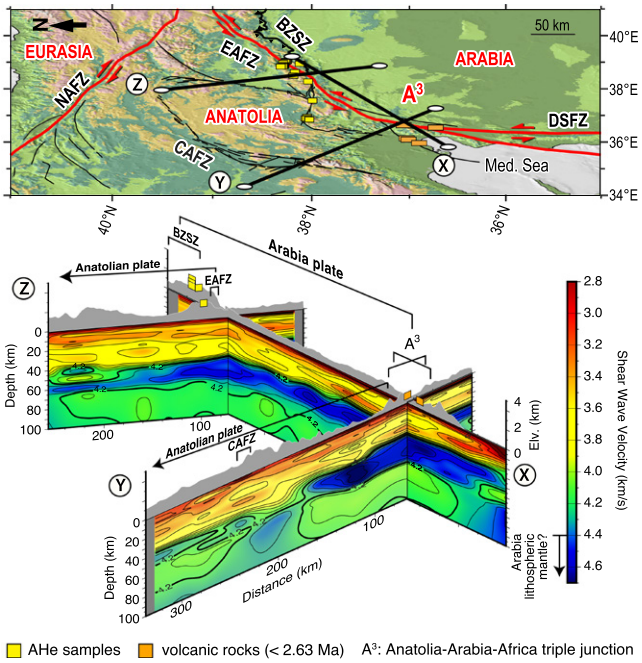

Figure 4. Cross sections along and across East Anatolian fault zone. Prominent high velocities (>4.4 km/s S-wave) are consistent with lithospheric mantle and are continuous with velocity structure of Arabian plate, extending northward well beyond Bitlis-Zagros suture zone and below Anatolian plate (Fig. 1B). These fast velocities are interpreted as rigid Arabian lithospheric mantle underthrusting Anatolian plate and represent a rheological boundary that likely contributed to location and formation of East Anatolian fault zone ca. 5 Ma. Elv—elevation; see Figure 1 caption for other acronym definitions.

Fig. S10), and they show clear continuity with the Arabian upper-mantle structure. Therefore, we interpret these fast upper-mantle seismic velocities to represent rigid lithospheric mantle underthrusting the slow (and therefore weak and/or thin-to-negligible) lithospheric mantle of the Anatolian plate. Indeed, geochemical evidence from basalts in the Anatolian plate indicates that a thin lithospheric mantle has existed below Anatolia since at least the mid-Miocene (Reid et al., 2019). The patterns of lithospheric mantle velocity structure today may reflect variations in the precollision geometry and structure of the northern Arabian margin.

DISCUSSION

Prior to the inception of the full escape system with the formation of the NAFZ and EAFZ, a broad region of Anatolia was deformed in response to Arabia-Eurasia collision (Albino et al., 2014; Darin et al., 2018; Umhoefer et al., 2020), initially in compression and later (by early Miocene) mostly under transtension (Kaymakçı et al., 2010). This phase of widespread distributed deformation driven by collision ("proto-escape") was protracted (ca. 23–5 Ma).

There was a major change in fault activity in many regions of the Arabia-Eurasia collision zone ca. 5 Ma (e.g., Allen et al., 2004). In addition, eastern Mediterranean marine basin sediments record a transition from thrusting to major subsidence at 5 Ma (Burton-Ferguson et al., 2005) related to a shift from contraction to transtension that is recorded up to the western border of submarine Arabian continental crust (Fig. 1A). The SE Anatolian plate boundary was dominated by strike-slip tectonics after ca. 5 Ma, when we propose that the EAFZ became a through-going structure linking the NAFZ and the Dead Sea fault zone (Fig. 1A). Rapid cooling following increased heat flow at ca. 5 Ma in the EAFZ is recorded by apatite He ages, coeval with the onset of basaltic volcanism (5–2.6 Ma) near the current location of the Anatolia-Arabia-Africa triple junction (Cosca et al., 2021; site of the 2023 M = 7.8 earthquake) and major rapid rearrangement of drainage systems within the uplifted Central Anatolian Plateau (Brocard et al., 2021), indicating that the transition to a strike-slip–dominated system was a regional phenomenon.

We interpret the young ages in and near the EAFZ to record heating driven by infiltration of hot fluids in fractured rock, as indicated by hot springs and travertine deposits (Duman and Emre, 2013). The geochemistry of thermal fluids in the EAFZ has a mantle signature, providing evidence for their deep-seated origin, even in fault segments not associated with magmatic activity (Italiano et al., 2013). The near-Euphrates traverse crosses a deep valley carved into fractured schist; the combination of focused erosion and fault-related infiltration of thermal fluids at temperatures high enough to reset apatite thermochronometers could explain the young ages in/near the EAFZ. Resetting of AHe and AFT ages by fault-related fluids has been documented in both strike-slip and normal faults (e.g., Wölfler et al., 2010).

The restriction of young ages to the vicinity of the EAFZ indicates its significance as a major structure starting ca. 5 Ma, which is >10–35 m.y. after the much-debated timing of Arabia-Eurasia collision. It is also long after the start of major extension in the Aegean (ca. 45 Ma), 10 m.y. after a significant increase in the rate of extension in the Aegean (ca. 15 Ma; Thomson et al., 1998), and at least 6–8 m.y. after tearing and break-off of the subducting slab below Anatolia (Reid et al., 2019).

Today, the inferred Arabia plate lithospheric mantle extends 100 ± 50 km north of the BZSZ under Anatolian crust (Figs. 1B and 4; Fig. S10). If we assume that this lithosphere was underthrust at a rate similar to modern convergence rates (~18 mm/yr), then the boundary was ~90 km south of its current location at 5 Ma, i.e., ~10 ± 50 km north of the suture. This significant rheological boundary at the margin of underthrust Arabian mantle likely facilitated localization of the EAFZ.

ESCAPE TECTONICS AND PLATE CREATION

Anatolia is ideal for evaluating how and over what time scale strike-slip faults become boundaries of a new plate. Lithosphere-scale strike-slip faults develop in orthogonal and oblique convergence but in most cases do not become plate-bounding structures. The development of an escape system, and therefore the creation of a plate such as Anatolia, requires a combination of collision and slab pull, with the latter related in part to mantle flow and slab dynamics, including tearing and fragmentation such as are observed in central Anatolia (e.g., Faccenna et al., 2014). The Ailao Shan–Red River shear zone in SE Asia may be analogous to the Anatolian escape structures in that it is an intracontinental fault zone at the edge of an orogenic plateau, connecting a convergence zone with extension in a marine basin (Leloup et al., 2001).

The Anatolian region had many factors facilitating the development of tectonic escape: high-angle indentation by Arabia, rheologically strong regions to the north and south, preexisting weak zones in favorable orientation relative to convergence, and ongoing extension in the west. Rheological boundaries controlled the locations of both major, ultimately plate-bounding, strike-slip faults. In the case of the EAFZ, the rheological boundary is between the Eurasian plate and the underthrusting strong Arabia plate lithospheric mantle, culminating in creation of the Anatolian plate at ca. 5 Ma.

ACKNOWLEDGMENTS

This research was funded by National Science Foundation grants "Continental Dynamics: Central Anatolian Tectonics" (CD-CAT) to Whitney and Teyssier (EAR-1109762); to Umhoefer (EAR-1109826); and to Thomson and Beck (EAR-1109336). Samples were collected by C. Lefebvre and analyzed with the assistance of P. Reiners. We thank U.S. Geological Survey reviewers N. Griffis and C. Sturrock and journal reviewers W. Cavazza, T. Schildgen, and two anonymous reviewers. Any use of trade, firm, or product names is for descriptive purposes only and does not imply endorsement by the U.S. government.

REFERENCES CITED

Abgarmi, B., Delph, J.R., Özacar, A.A., Beck, S.L., Zandt, G., Sandvol, E., Türkelli, N., and Biryol, C.B., 2017, Structure of the crust and African

slab beneath the Central Anatolian Plateau from receiver functions: New insights on isostatic compensation and slab dynamics: Geosphere, v. 13, p. 1774–1787, https://doi.org/10.1130/GES01509.1.

Albino, I., Cavazza, W., Zattin, M., Okay, A.I., Adamia, S., and Sadradze, N., 2014, Far-field tectonic effects of the Arabia-Eurasia collision and the inception of the North Anatolian fault system: Geological Magazine, v. 151, p. 372–379, https://doi.org/10.1017/S0016756813000952.

Allen, M.B., Jackson, J., and Walker, R., 2004, Late Cenozoic reorganization of the Arabia-Eurasia collision and the comparison of short-term and long-term deformation rates: Tectonics, v. 23, TC2008, https://doi.org/10.1029/2003TC001530.

Brocard, G.Y., Meijers, M.J.M., Cosca, M.A., Salles, T., Willenbring, J., Teyssier, C., and Whitney, D.L., 2021, Fast integration of the Central Anatolian Plateau drainage driven by Pliocene surface uplift and escape tectonics: Geosphere, v. 17, p. 739–765, https://doi.org/10.1130/GES02247.1.

Bulut, F., Bohnhoff, M., Eken, T., Janssen, C., Kılıç, T., and Dresen, G., 2012, The East Anatolian fault zone: Seismotectonic setting and spatiotemporal characteristics of seismicity based on precise earthquake locations: Journal of Geophysical Research, v. 117, B07304, https://doi.org/10.1029/2011JB008966.

Burke, K., and Şengör, A.M.C., 1986, Tectonic escape in the evolution of the continental crust, *in* Barazangi, M., and Brown, L., eds., Reflection Seismology: The Continental Crust: American Geophysical Union Geodynamics Monograph 14, p. 41–53, https://doi.org/10.1029/GD014p0041.

Burton-Ferguson, R., Aksu, A.E., Calon, T.J., and Hall, J., 2005, Seismic stratigraphy and structural evolution of the Adana Basin, eastern Mediterranean: Marine Geology, v. 221, p. 189–222, https://doi.org/10.1016/j.margeo.2005.03.009.

Cavazza, W., Catto, S., Zattin, M., Okay, A.I., and Reiners, P., 2018, Thermochronology of the Miocene Arabia-Eurasia collision zone of southeastern Turkey: Geosphere, v. 14, p. 2277–2293, https://doi.org/10.1130/GES01637.1.

Cosca, M.A., Reid, M., Delph, J.R., Gençalioğlu Kuşcu, G., Blichert-Toft, J., Premo, W., Whitney, D.L., Teyssier, C., and Rojay, B., 2021, Age and mantle sources of Quaternary basalts associated with "leaky" transform faults of the migrating Anatolia-Arabia-Africa triple junction: Geosphere, v. 17, p. 69–94, https://doi.org/10.1130/GES02266.1.

Darin, M.H., Umhoefer, P.J., and Thomson, S.N., 2018, Rapid late Eocene exhumation of the Sivas Basin (central Anatolia) driven by initial Arabia-Eurasia collision: Tectonics, v. 37, p. 3805–3833, https://doi.org/10.1029/2017TC004954.

Delph, J.R., Abgarmi, B., Ward, K.M., Beck, S.L., Özacar, A.A., Zandt, G., Sandvol, E., Türkelli, N., and Kalafat, D., 2017, The effects of subduction termination on the continental lithosphere: Linking volcanism, deformation, surface uplift, and slab tearing in central Anatolia: Geosphere, v. 13, p. 1788–1805, https://doi.org/10.1130/GES01478.1.

Duman, T.Y., and Emre, O., 2013, The East Anatolian fault: Geometry, segmentation and jog characteristics, *in* Robertson, A.H.F., et al., eds., Geological Development of Anatolia and the Easternmost Mediterranean Region: Geological Society, London, Special Publication 372, p. 495–529, https://doi.org/10.1144/SP372.14.

Faccenna, C., Becker, T.W., Jolivet, L., and Keskin, M., 2013, Mantle convection in the Middle East: Reconciling Afar upwelling, Arabia indentation and Aegean trench rollback: Earth and Planetary Science Letters, v. 375, p. 254–269, https://doi.org/10.1016/j.epsl.2013.05.043.

Faccenna, C., Becker, T.W., Auer, L., Billi, A., Boschi, L., Brun, J.-P., Capitanio, F., Funicello, F., Horvàth, F., Jolivet, L., Piromallo, C., Royden, L., Rossetti, F., and Serpelloni, E., 2014, Mantle dynamics in the Mediterranean: Reviews of Geophysics, v. 52, p. 283–332, https://doi.org/10.1002/2013RG000444.

He, J., Thomson, S.N., Reiners, P.W., Hemming, S.R., and Licht, K.J., 2021, Rapid erosion of the central Transantarctic Mountains at the Eocene-Oligocene transition: Evidence from skewed (U-Th)/He date distributions near Beardmore Glacier: Earth and Planetary Science Letters, v. 567, https://doi.org/10.1016/j.epsl.2021.117009.

Italiano, F., Sasmaz, A., Yuce, G., and Okan, O., 2013, Thermal fluids along the East Anatolian fault zone (EAFZ): Geochemical features and relationships with tectonic setting: Chemical Geology, v. 339, p. 103–114, https://doi.org/10.1016/j.chemgeo.2012.07.027.

Karaoğlan, F., Parlak, O., Heil, E., and Klötzli, U., 2016, The temporal evolution of the active margin along the Southeast Anatolian orogenic belt (SE Turkey): Evidence from U-Pb, Ar-Ar and fission track chronology: Gondwana Research, v. 33, p. 190–208, https://doi.org/10.1016/j.gr.2015.12.011.

Kaymakçı, N., Inceöz, M., Ertepınar, P., and Koç, A., 2010, Late Cretaceous to recent kinematics of SE Anatolia (Turkey), *in* Sosson, M., et al., eds., Sedimentary Basin Tectonics from the Black Sea and Caucasus to the Arabian Platform: Geological Society, London, Special Publication 340, p. 409–435, https://doi.org/10.1144/SP340.18.

Leloup, P.H., Arnaud, N., Lacassin, R., Kienast, J.R., Harrison, T.M., Trong, T.T.P., Replumaz, A., and Tapponnier, P., 2001, New constraints on the structure, thermochronology, and timing of the Ailao Shan–Red River shear zone, SE Asia: Journal of Geophysical Research, v. 106, p. 6683–6732, https://doi.org/10.1029/2000JB900322.

McKenzie, D.P., 1976, The East Anatolian fault: A major structure in eastern Turkey: Earth and Planetary Science Letters, v. 29, p. 189–193, https://doi.org/10.1016/0012-821X(76)90038-8.

Meijers, M.J., Brocard, G.Y., Cosca, M.A., Lüdecke, T., Teyssier, C., Whitney, D.L., and Mulch, A., 2018, Rapid late Miocene surface uplift of the Central Anatolian Plateau margin: Earth and Planetary Science Letters, v. 497, p. 29–41, https://doi.org/10.1016/j.epsl.2018.05.040.

Molnar, P., and Dayem, K.E., 2010, Major intracontinental strike-slip faults and contrasts in lithospheric strength: Geosphere, v. 6, p. 444–467, https://doi.org/10.1130/GES00519.1.

Muehlberger, W.R., and Gordon, M.B., 1987, Observations on the complexity of the East Anatolian fault, Turkey: Journal of Structural Geology, v. 9, p. 899–903, https://doi.org/10.1016/0191-8141(87)90091-5.

Okay, A.I., Zattin, M., and Cavazza, W., 2010, Apatite fission-track data for the Miocene Arabia-Eurasia collision: Geology, v. 38, p. 35–38, https://doi.org/10.1130/G30234.1.

Okay, A.I., Zattin, M., Özcan, E., and Sunal, G., 2020, Uplift of Anatolia: Turkish Journal of Earth Sciences, v. 29, p. 696–713, https://doi.org/10.3906/yer-2003-10.

Reid, M.R., Delph, J.R., Cosca, M.A., Schleiffarth, W.K., and Gençalioğlu Kuşcu, G., 2019, Melt equilibration depths as sensors of lithospheric thickness during Eurasia-Arabia collision and the uplift of the Anatolian Plateau: Geology, v. 47, p. 943–947, https://doi.org/10.1130/G46420.1.

Reilinger, R., et al., 2006, GPS constraints on continental deformation in the Africa-Arabia-Eurasia continental collision zone and implications for the dynamics of plate interactions: Journal of Geophysical Research–Solid Earth, v. 111, B05411, https://doi.org/10.1029/2005JB004051.

Rojay, B., Heimann, A., and Toprak, V., 2001, The transition zone between the Dead Sea transform and the East Anatolian fault zone: Geodinamica Acta, v. 14, p. 197–212, https://doi.org/10.1080/09853111.2001.11432444.

Schildgen, T.F., Yıldırım, C., Cosentino, D., and Strecker, M.R., 2014, Linking slab break-off, Hellenic trench retreat, and uplift of the Central and Eastern Anatolian Plateaus: Earth-Science Reviews, v. 128, p. 147–168, https://doi.org/10.1016/j.earscirev.2013.11.006.

Şengör, A.M.C., Tüysüz, O., İmren, C., Sakınç, M., Eyidoğan, H., Görür, N., Le Pichon, X., and Rangin, C., 2005, The North Anatolian fault: A new look: Annual Reviews in Earth and Planetary Sciences, v. 33, p. 37–112, https://doi.org/10.1146/annurev.earth.32.101802.120415.

Tackley, P.J., 2000, Self-consistent generation of tectonic plates in time-dependent, three-dimensional mantle convection simulations: 1. Pseudoplastic yielding: Geochemistry, Geophysics, Geosystems, v. 1, 1021, https://doi.org/10.1029/2000GC000036.

Tapponnier, P., Peltzer, G., Le Dain, A.Y., Armijo, R., and Cobbold, P., 1982, Propagating extrusion tectonics in Asia: New insights from simple experiments with plasticine: Geology, v. 10, p. 611–616, https://doi.org/10.1130/0091-7613(1982)10<611:PETIAN>2.0.CO;2.

Thomson, S.N., Stockhert, B., and Brix, M.R., 1998, Thermochronology of the high-pressure metamorphic rocks of Crete, Greece: Implications for the speed of tectonic processes: Geology, v. 26, p. 259–262, https://doi.org/10.1130/0091-7613(1998)026<0259:TOTHPM>2.3.CO;2.

Umhoefer, P.J., Lefebvre, C., Thomson, S.N., Cosca, M.A., Teyssier, C., and Whitney, D.L., 2020, Cenozoic tectonic evolution of a reactivated suture zone during the transition from Arabia-Eurasia collision to escape tectonics: The Ecemiş fault and adjacent basins, central Anatolia, Turkey: Geosphere, v. 16, p. 1358–1384, https://doi.org/10.1130/GES02255.1.

Wölfler, A., Kurz, W., Danisik, M., and Rabitsch, R., 2010, Dating of fault zone activity by apatite fission track and apatite (U-Th)/He thermochronometry: A case study from the Lavanttal fault system (eastern Alps): Terra Nova, v. 22, p. 274–282, https://doi.org/10.1111/j.1365-3121.2010.00943.x.

Printed in USA